Journal of Solid State Chemistry **157,** 296–308 (2001)
doi:10.1006/jssc.2000.9065, available online at http://www.idealibrary.com on IDEAL®

Experimental Study of Structure–Energy Changes in Molecules and Crystals of 2,2-Dinitropropane-1,3-diol Caused by Temperature Variations

N. I. Golovina,[1] A. V. Raevskii, B. S. Fedorov, I. G. Gusakovskaya, R. F. Trofimova, N. V. Chukanov, S. A. Vozchikova, G. V. Shilov, V. P. Tarasov, L. N. Erofeev, and L. O. Atovmyan

Institute of Problems of Chemical Physics, Russian Academy of Sciences, 142432 Chernogolovka, Moscow Region, Russian Federation

Received June 20, 2000; in revised form November 21, 2000; accepted December 8, 2000; published online February 19, 2001

Crystals of 2,2-dinitropropane-1,3-diol were prepared and grown at different temperatures. An X-ray analysis was used to study the structure of three phases (1, 2 and 3) of the 2,2-dinitropropane-1,3-diol crystals. The calorimetric study of the crystals temperature behavior (1) showed the presence of two phase transitions in the regions of $T = 309$ K and $T = 340$ K, as well as crystals (2) with a phase transition at $T = 340$ K. Observations in a hot stage with the optical microscope phase transitions for separate crystals were made. X-ray diffraction studies of polycrystalline samples (1) for temperatures increasing up to the temperatures of phase transitions I and II demonstrated that phase transition I is followed by conversion of crystals 1 into 2, and transition II is connected with conversion of crystals 2 into a disordered body-centered structure. The temperature behavior of the bands of symmetric N–O stretching vibrations of nitro groups and stretching vibrations of O–H groups was studied by IR spectroscopy. The temperature dependence of hydrogen bonds redistribution and nitro group reorientational dynamics was examined. Data on the structure–dynamic rearrangement in the crystal lattice of the examined compound were obtained by the NMR pulse method in the solid phase using relaxational free induction decay of protons. The kinetic parameters of the process were obtained.

INTRODUCTION

This work is a continuation of our studies (1, 2) on structure–energy conversions in crystals formed by molecules with a number of various functional groups. Temperature-dependent structural properties of such crystals may be determined by intermolecular forces (van der Waals interactions, hydrogen bonds, exchange interactions) and complex combinations of energy redistribution between different degrees of freedom within the multifunctional molecule itself and, naturally, by combination of intra- and intermolecular interactions. Since the temperature dependences are different for each type of interactions, this leads to complicated changes of the molecule state because of redistribution of interactions during temperature variations. Energy redistribution affects the bond length changes and leads to new degrees of freedom of functional groups (change of entropy factor); generally speaking, it changes the molecular reactivity as a whole. Crystals of 2,2-dinitropropane-1,3-diol (DNPD), whose molecules are symmetric and have two interacting nitro groups at a central carbon atom and two relatively free end hydroxylic groups binding the molecules by hydrogen bonds in a condensed phase, were chosen for investigation. Two nitro groups at one carbon may be bound with each other through dipole–dipole and orbital interactions. Previously we showed, on the basis of the crystallochemical investigation and study of UV spectra of polynitro compounds (3), that nonbonded n_σ–π^* orbital interaction between the nitro groups may also exist for the molecules containing two or more nitro groups, along with an electrostatic $O^- \cdots N^+$ interaction between them leading to their polarization. The n_σ–π^* interaction leads to additional polarization of NO_2 groups, and to shortening of nonbonded $O \cdots N$ contacts, as well as to almost orthogonal arrangement of the nitro groups' planes in the molecule. At the same time, the conformational calculations of molecules having a dinitromethylene group, which are done without considering electrostatic and nonbonded orbital interactions, give an angle between the nitro groups planes close to 55°. The DNPD molecule under examination with a central dinitromethylene group may have both interactions between the nitro groups and interactions of the nitro groups with the polar $C^{\delta+}$–$O^{\delta-}$ bonds; the molecules conformation changes with

[1]To whom correspondence should be addressed: Fax: + 7(096)5155420. E-mail: niv@icp.ac.ru.

0022-4596/01 $35.00

a temperature increase should be controlled by the energy values of different interactions.

EXPERIMENTAL

2,2- Dinitropropane-1,3-diol was prepared from dinitromethane potassium salt and formaldehyde in the presence of acetic acid according to a known technique (4).

$$K^+CH(NO_2)_2 + CH_2O + AcOH \xrightarrow[H_2O]{} HOCH_2C(NO_2)_2CH_2OH + AcOK.$$

The product obtained was dried over P_2O_5 after being filtered and twice recrystallized, first from benzene and then from anhydrous dichloroethane. The recrystallization was carried out as follows: a weighed portion of the substance in the crystallizer with an attached anchor mixer was warmed in anhydrous dichloroethane (1 g of the substance per 15 ml of DCE) to boiling. The prepared solution was cooled at a rate of 0.1–0.2 deg/min at a mixer rotation speed of 43–45 rotations/min down to 327–329 K. On reaching this temperature, the rotation was stopped and the crystallization process went spontaneously to $T \approx 293$ K at a cooling rate of 0.2–0.4 deg/min. Colorless needles were filtered off that were dried in air in a flow of dry nitrogen. The prepared crystals of 2,2-dinitropropane-1,3-diol (**1**) with m.p. 410.5–412 K were then investigated with different physical methods. 2,2-Dinitropropane-1,3-diol was prepared by using the same technique (4), but was twice recrystallized from dichloroethane. It was formed crystals (**2**) with m.p. 412–413 K that were also examined by the physical methods.

TABLE 1
Crystal Data of the 1, 2, and 3–$C_3H_6N_2O_6$ Structures

Unit cell parameters	Structure		
	1	**2**	**3**
a (Å)	11.774(5)	9.767(2)	6.070(40)
b (Å)	9.568(4)	11.253(6)	9.769(61)
c (Å)	5.802(2)	6.076(3)	11.251(35)
β (°)	96.25(7)	90.00	90.00
V (Å^3)	649.8(6)	667.9(5)	667.3(9)
d_{calc} (g/cm^3)	1.697(3)	1.651(2)	1.652(9)
Space group	$P2_1/n$	$P2_12_12_1$	$P2_12_12_1$
z	4	4	4
λ (Å)	0.7092	1.5486	0.7092
μ (mm^{-1})	0.163	1.464	0.163
M	166.091	166.091	166.091
Number of reflns. $> 2\sigma$	952	538	438
R	0.064	0.074	0.064

TABLE 2
Atomic Coordinates (10^4) in Structure 1, $C_3H_6N_2O_6$

Atom	X	Y	Z
O(1)	8892(2)	4059(2)	6916(3)
O(2)	7208(2)	4234(2)	5094(4)
O(3)	7342(2)	2842(2)	473(3)
O(4)	6621(2)	1446(3)	2810(5)
O(5)	9669(2)	1620(2)	1401(3)
O(6)	9611(2)	1001(2)	6831(3)
N(1)	8134(2)	3683(2)	5471(3)
N(2)	7365(2)	2226(2)	2295(4)
C(1)	9459(2)	2731(2)	2852(4)
C(2)	8406(2)	2417(2)	4072(4)
C(3)	8523(2)	1112(2)	5633(3)
H(1)	9881(30)	909(30)	2227(70)
H(2)	9583(30)	1206(40)	8253(60)
H(3)	9333(30)	3574(40)	1954(40)
H(4)	10107(20)	2882(20)	3982(60)
H(5)	7961(20)	1149(30)	6725(50)
H(6)	8363(30)	287(30)	4695(40)

1. An X-Ray Study

The structure of the two phases of the 2,2-dinitropropane-1,3-diol crystals **1** and **2** was studied at room temperature. The structure of the crystals **3** grown from the phase **1** solution in dichloroethane was studied at $T = 306$ K in a hot stage using an optical microscope. The crystal data of the structures are given in Table 1. The reflection intensities were recorded in the range $0.02 \leq \sin\theta/\lambda \leq 0.55$ on a four-circle KM-4 (KUMA-Diffraction, Poland) diffractometer using a $\omega/2\theta$ scanning technique. The structures were refined by direct methods using

TABLE 3
Atomic Coordinates ($\times 10^4$) in Structure 2, $C_3H_6N_2O_6$

Atom	X	Y	Z
O(1)	5342(20)	8293(10)	4994(20)
O(2)	4057(10)	7163(10)	6966(20)
O(3)	3009(10)	7114(10)	1969(20)
O(4)	3085(10)	5222(10)	2483(30)
O(5)	6523(8)	5470(8)	6210(20)
O(6)	6145(8)	5768(7)	521(10)
N(1)	4719(10)	7369(10)	5348(20)
N(2)	3534(10)	6209(10)	2669(20)
C(1)	5302(10)	5245(10)	5029(20)
C(2)	4933(9)	6361(9)	3746(20)
C(3)	5955(10)	6702(10)	1981(20)
H(1)	4553(150)	5020(120)	5989(240)
H(2)	5436(130)	4569(120)	4022(230)
H(3)	5599(140)	7397(120)	1191(220)
H(4)	6792(150)	6938(100)	2658(230)
H(5)	6324(130)	5550(120)	7602(280)
H(6)	6898(160)	5406(120)	815(220)

TABLE 4
Atomic Coordinates ($\times 10^4$) in Structure 3, $C_3H_6N_2O_6$

Atom	*X*	*Y*	*Z*
O(1)	−148(14)	5410(18)	3254(7)
O(2)	−2052(17)	3987(18)	2271(10)
O(3)	3108(20)	2944(17)	2016(14)
O(4)	2364(20)	3064(10)	227(10)
O(5)	−1211(15)	6507(12)	442(9)
O(6)	4481(14)	6105(14)	771(9)
N(1)	−514(16)	4656(14)	2386(8)
N(2)	2299(20)	3652(10)	1205(8)
C(1)	−17(14)	5218(8)	189(6)
C(2)	1253(17)	4943(10)	1508(9)
C(3)	2883(17)	6129(20)	1762(9)
H(1)	939(130)	5399(60)	−443(70)
H(2)	−1044(130)	4558(70)	47(60)
H(3)	4286(140)	6621(80)	394(70)
H(4)	−2715(140)	6214(70)	368(60)
H(5)	2211(150)	6835(80)	1913(80)
H(6)	3698(130)	5673(70)	2424(70)

a system of SHELX-86 program on a PC. The atomic coordinates in structures **1**, **2**, and **3** (Tables 2–4) were refined by a full-matrix approximation using the SHELXL-93 program; the refinement for nonhydrogen atoms was carried out in an anisotropic approximation and that for hydrogen atoms in an isotropic approximation.

Structures **1** and **2** belong to different space groups (Table 1). In the centrosymmetric structure **1**, the DNPD molecules are symmetric, but not planar; hence they are represented both by left and right forms (Fig. 1). At the same time, structures **2** and **3** are axial, and their DNPD molecules may be either right or left (Fig. 2). Newman projections calculated for the molecules of the structures **1**, **2**, and **3** (Figs. 3–6) show that molecules **2** and **3** are optical antipodes. The molecular conformation in structure **1** (Fig. 3) is stabilized by electrostatic dipole–dipole and orbital interactions between the nitro groups, as well as orbital interactions between one of the nitro groups and C–O polar bonds. Such a conclusion can be drawn from the mutual arrangement of the molecule fragments: the dihedral angle between

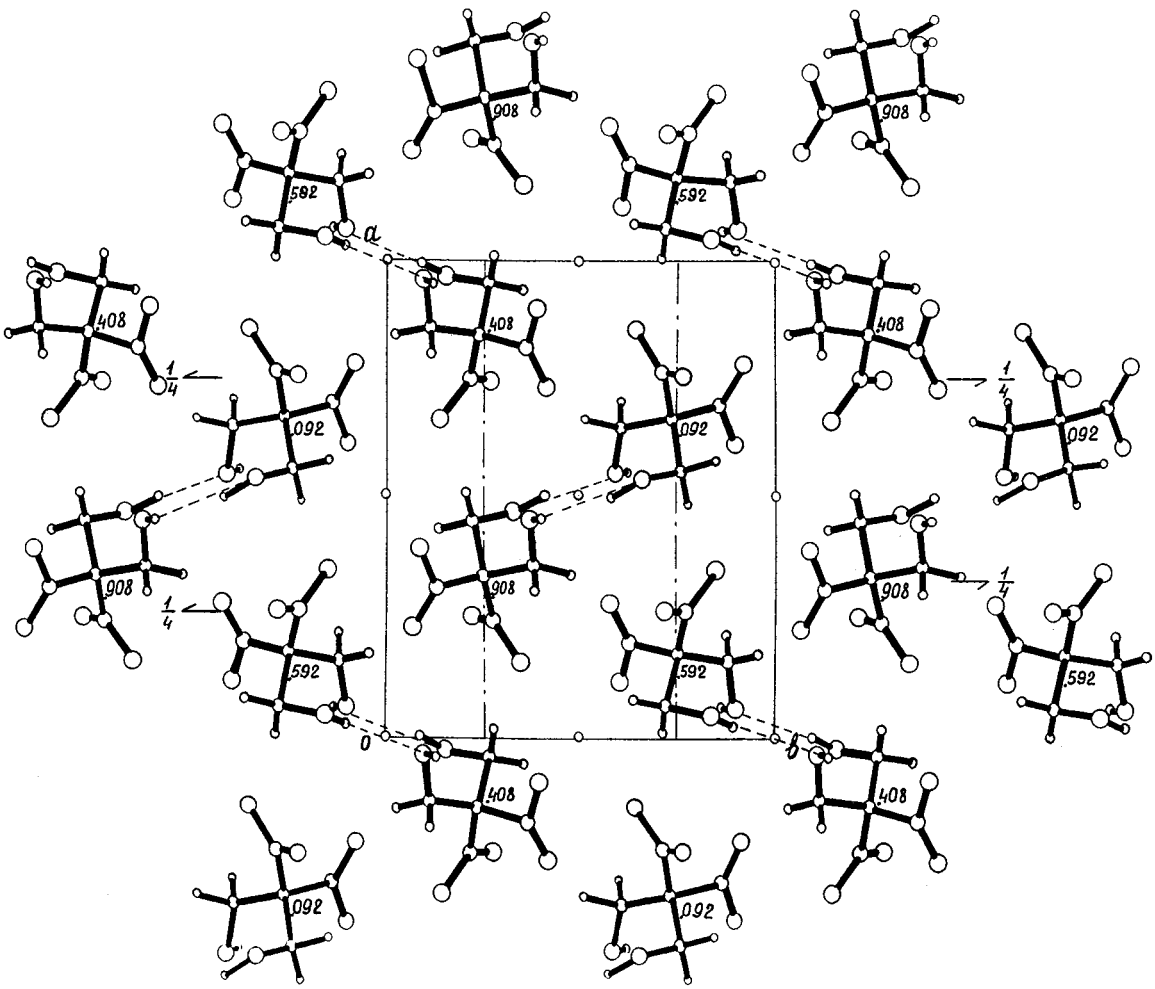

FIG. 1. Projection of structure **1** on the plane (*ab*).

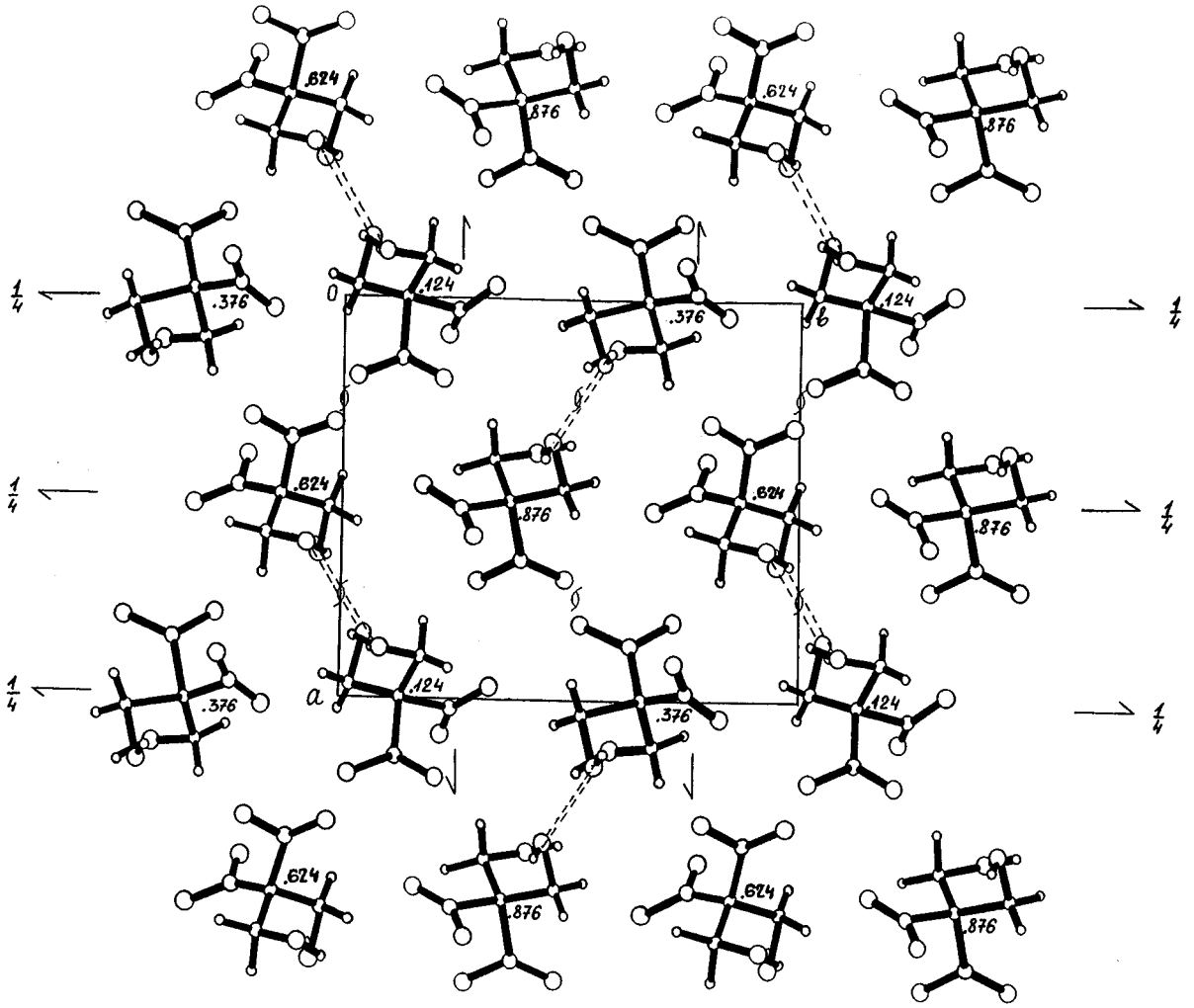

FIG. 2. Projection of structure **2** on the plane (*ab*).

the nitro group planes is 89.8° and the distance $O(2)\cdots N(2) = 2.550$ Å, which corresponds to an orbital interaction of the $n(NO_2) \rightarrow \pi^*(NO_2)$ type between the N(1)O(1)O(2) and N(2)O(3)O(4) nitro groups. The $O(2)^- \cdots N(2)^+$ electrostatic interaction between them acts in the same direction. The mutual arrangement of the C(2)N(2)O(3)O(4) and C(2)C(1)O(5) planes, as well as the C(2)N(2)O(3)O(4) and C(2)C(3)O(6) planes with angles of 106.4 and 25.0° and short contacts $C(1)\cdots O(3) = 2.716(8)$ Å and $C(3)\cdots O(4) = 2.642(7)$ Å in addition to the angles between the C(2)N(2) and C(1)O(5) lines, 71.7°, as well as between C(2)N(2) and C(3)O(6), 16.9°, accounts for orbital interactions between lone electron pairs of the N(2)O(3)O(4) nitro group and σ^* vacant orbitals of the C–O bonds. In the first case, it is an $n(NO_2) \rightarrow \sigma^*$[C(1)–O(5)] interaction; in the second case, it is a $\pi(NO_2) \rightarrow \sigma^*$[C(3)–O(6)] interaction. All the nonvalent interactions in molecule **1** stabilize the observed conformation. The conformation of molecules **2** and **3** (Figs. 4 and 5) is different from that examined above. In the case of molecule **3**, the angle between the nitro group planes became smaller, 82.6°, the distance between atoms $(O3)\cdots(N1)$ having increased to 2.683 Å, which obviously demonstrates decreased orbital and electrostatic interactions between the nitro groups. The character of the nitro groups, interaction with the C–O bonds is also changed: now each nitro group interacts with a separate C–O bond. Thus the C(2)N(1)O(1)O(2) nitro group plane makes an angle of 5.5° with the C(2)C(3)O(6) plane, having a distance $O(1)\cdots C(3) = 2.594(7)$ Å and an angle between the C(2)N(1) and C(3)O(6) lines 178.5°, which suggests a probable $n(NO_2) \rightarrow \sigma^*$[C(3)–O(6)] orbital interaction. The C(2)N(2)O(3)O(4) nitro group plane makes an angle of 22.0° with the C(2)C(1)O(5) plane, having a distance $O(4)\cdots C(1) = 2.634(8)$ Å and an angle between the C(2)N(2) and C(1)O(5) lines 172.1°, which may also speak

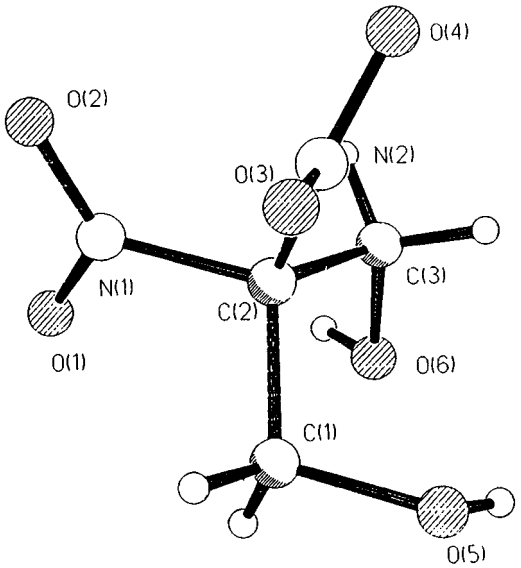

FIG. 3. Molecule **1**.

of a possible $n(NO_2) \rightarrow \sigma^*[C(1)–O(5)]$ orbital interaction. The conformation of molecule **2** is almost identical to the conformation of molecule **3**. Thus, the dinitromethylene group possesses two energy states corresponding to two different conformations of the DNPD molecule. The stress–strain energy calculations in the molecule with consideration of the dipole–dipole interaction but not taking into account orbital interactions using the MMX (5) program show that the energy of molecule **1** is 1.12 kcal/mol more favorable than that of molecule **3**. At the same time, the energy calculations of the structure by the atom–atom potentials method with allowance made for hydrogen bond energy show that the structures of crystals **1** and **3** are close in energy; for the crystal **1** structure, the total energy is

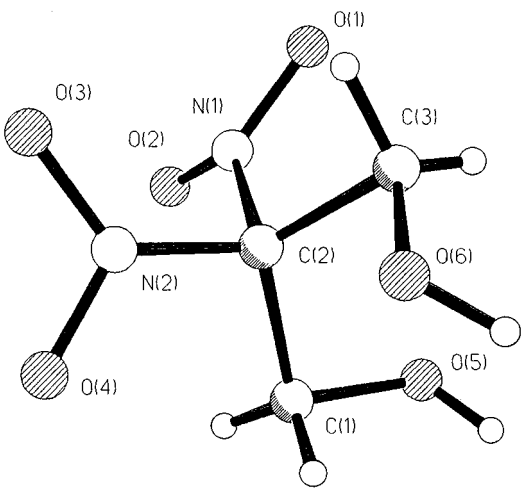

FIG. 4. Molecule **2**.

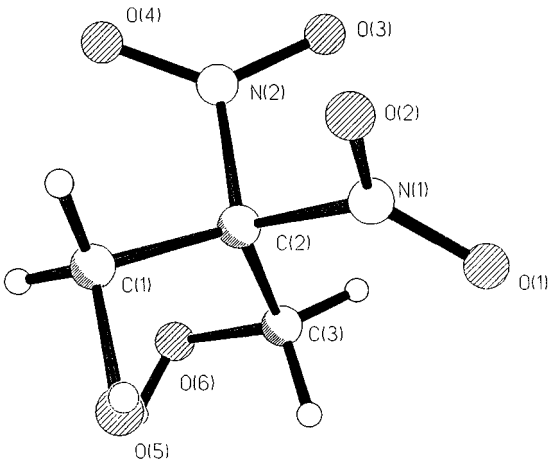

FIG. 5. Molecule **3**.

$E = -15.669$ kcal/mol and the hydrogen bonds energy is -4.467 kcal/mol, while for the crystals **3** structure, $E = -15.613$ kcal/mol and the hydrogen bonds energy is -5.470 kcal/mol. Taking everything in consideration structure **1** is 1.17 kcal/mol more favorable than structure **3**. It should be noted that in both structures the hydrogen bonds form infinite chains; in structure **1**, they are directed along the *c* axis with the distance $O(5) \cdots O(6) = 2.704$ Å and the short distance between the chains $O(5) \cdots O(6) = 2.794$ Å (Fig. 1). In structure **3**, the chains are also directed along the *c* axis, with the distance $O(5) \cdots O(6) = 2.669$ Å inside the chain and the short distance $O(5) \cdots O(6) = 2.735$ Å between them (Fig. 2).

No diversity is observed in the equivalent bond lengths in molecules **1** and **3** due to the differences in the character of orbital interactions. However, in molecule **3** (crystals **3** were grown at 306 K), there are noticeable differences in the N–O bond lengths within each nitro group (1.21(1)–1.24(1) Å).

2. Temperature X-Ray Diffraction Studies

The temperature X-ray diffraction studies of the DNPD single crystals proved impossible as crystals **1** disintegrated near 308 K and crystals **2** near 340 K. Hence, the temperature investigations were performed on polycrystal samples placed in the variable-temperature cell of a DRON-M diffractometer (temperature accuracy $\pm 2°$). The counting was done at a rate of 2 deg/min. Theoretic powder patterns were previously calculated on the basis of the results of investigation of structures **1** and **2**. The diffraction pattern of the polycrystal samples at room temperature completely corresponds to the one calculated for structure **1**, as does the diffraction pattern recorded at $T = 318$ K with that calculated for structure **2**. As a result it is proved that phase transition I corresponds to a transition of crystals **1** into **2**, i.e., from a monoclinic phase into an orthorhombic one. The

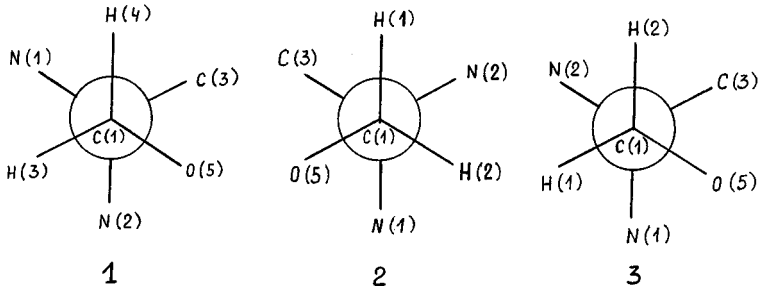

FIG. 6. Newman projection for molecules **1**, **2**, and **3**.

diffraction pattern of the same type at $T = 348$ K shows the presence of one more phase transition: The position of four indexed lines given in Table 5 allows us to refer the crystals after transition II (i.e., for $T > T_{kII}$) to a body-centered cubic structure with a period of $a = 10.101$ Å.

Reconstruction of transition I can be performed after superimposing structure **1** on structure **2** (Figs. 1 and 2), the beginning of the coordinates being shifted in structure **2** by $0.5b$ along the x axis (**1**) and by $0.25c$ along the z axis (**1**). There are coincident and noncoincident layers in both the structures. And a full coincidence of the positions of all atoms in molecules is observed in the coincident layers (the layer thickness is $0.5a$ in structure **1** and $0.5b$ in structure **2**), while in the noncoincident layers, the molecules serve as antipodes to each other and their centers of gravity are noncoincident along the c axis. That means that the following changes occur in the range 306.5–314 K in structure **1** during the first transition. First, the dinitromethylene group turns relative to the –C–C–C– carcass of the molecule with a simultaneous turn of the $-CH_2-OH$ fragments about the C–C bonds corresponding to the left–right forms transitions of the molecule; i.e., the molecule passes to a new conformational level. In phase **2** only the molecules of one form stand out (either right or left) with a new mode of molecular packing and a new arrangement of hydrogen bonds. During transition II, transforming a structure into a cubic phase, the molecules lose their individuality, turning into spheroids, which is caused by a definite type of the motion of a molecule as a whole. In a cubic phase we observe sharp diffraction peaks. It should be noted that the cubic phase diffraction peaks appear at $T = 333$ K, i.e., before the moment of phase transition at $T = 340$ K.

TABLE 5
Diffractogram of Polycrystals 1 at $T = 348$ K

hkl	2θ	$\sin\theta$	d (Å)	a (Å)
200 weak	17.0	0.1478	5.215	10.430
220 weak	27.9	0.2394	3.164	10.014
222 very strong	31.2	0.2689	2.867	9.931
004 strong	35.8	0.3074	2.508	10.031

3. Microscope Observations of the Phase Transitions on the DNPD Single Crystals

Investigations in a hot stage using an optic microscope (the Nu-2 instrument, Karl Zeiss, Iena) were made under polarized light and constant heating at a rate of $\sim$1deg/min. The temperature accuracy was $\pm 1^\circ$. The initial DNPD crystals were elongated, quite defective, transparent optically active crystals with dimensions of up to $1 \times 1 \times 10$ mm^3.

During the first heating, at about 310 K the first phase transition was observed against variation of optical activity. Usually it started in the vicinity of the most defective regions and spread as a reaction front with a width of about 30 μm throughout the whole crystal. In different crystals the phase transition started at different temperatures, and the scatter of temperatures at which the transition began reached 10°. The rate of phase transfer in each crystal remained the same. As the temperature increased, the optical activity of the crystals varied gradually, until on reaching 342 K, there occurred a fast second phase transition from an optically active phase into an isotropic (cubic) phase not possessing optical activity. In this case, there was also a scatter in the temperatures at which the phase transition began reaching a few degrees. On cooling, all the phases showed significant overcooling. Thus, the cubic phase was retained up to 303 K, while the orthorhombic one survived at room temperature during the whole period of observation if the crystal was not subjected to any mechanical attack. After the crystal was acted upon (e.g., taken with pincers), the phase transition from an orthorhombic phase into a monoclinic phase occurred. So the microscope observations showed the following:

(1) The DNPD crystals undergo two phase transitions: the first (I) at $\sim$310 K and the second (II) at $\sim$342 K, the first phase transition is from an anisotropic (monoclinic) phase to an anisotropic (orthorhombic) phase, and the second from an anisotropic (orthorhombic) into an isotropic (cubic) phase.

(2) The temperature of phase transitions I and II may differ by a few degrees because of the influence of crystal lattice defects on the beginning of the phase transition, i.e., on the temperature of phase overheating.

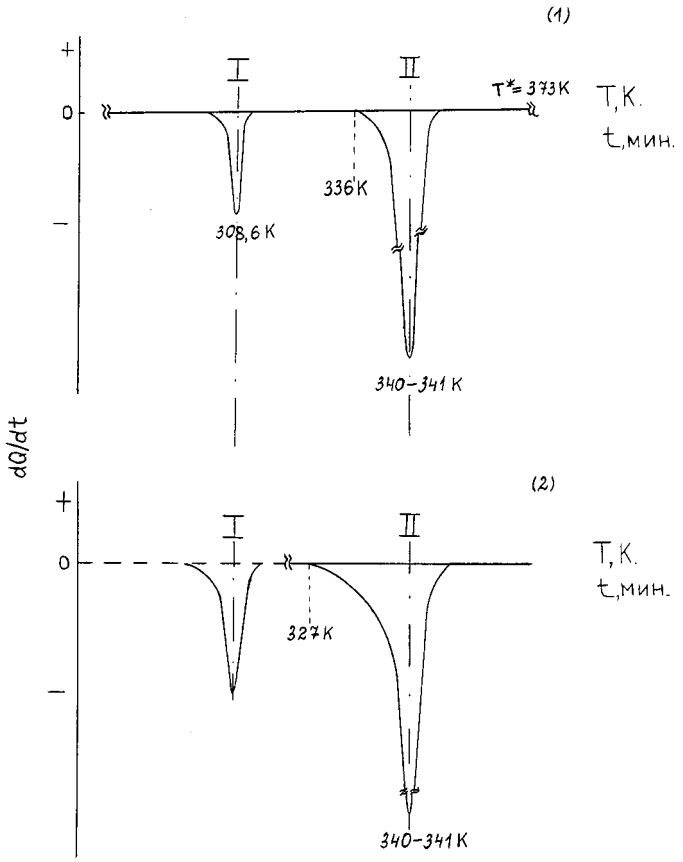

FIG. 7. Dependence of heat consumption rate, dQ/dt, on temperature T and time t (thermograms) during heating to 273 K ($V \approx 0.1$ deg/min) of crystals **1** pressed in a calorimetric cell. (1) $Q_{\mathrm{I}} = -0.8$ kcal/mol $\pm$ 5%; $Q_{\mathrm{II}} = -6$ kcal/mol $\pm$ 5%. (2) Expansion of the temperature region of the transition II prephase state with increasing method sensitivity. (The thermograms are qualitative, the time is not indicated on the abscissa).

(3) For the existing phases, there is a possibility of considerable overheating that allows a decrease by tens of degrees for the temperature of a reverse phase transition.

4. *Calorimetric Studies*

2,2-Dinitropropane-1,3-diol crystals **1** and **2** were studied on a scanning Calvet type microcalorimeter in the temperature range 303–373 K. Two phase transitions I and II at $T_{\mathrm{kI}} = 308.6$ K and $T_{\mathrm{kII}} = 341$ K are found in calorimetric investigations of polycrystals **1** of this substance for an approximately 0.1–0.2 deg/min heating rate in the 303–373 K temperature range. The thermogram of heating is given in Fig. 7: $Q_{\mathrm{I}} = -0.764$ kcal/mol and $Q_{\mathrm{II}} = -5.994$ kcal/mol. On repeated heating of this sample from 303 K to 473 K, thermogram 7(1) occurs over and over again if the temperature T^* from which the sample is cooled after heating exceeds T_{kII}, i.e., under the condition that $T^* > T_{\mathrm{kII}}$.

It is believed (on the basis of the structural data) that transition I is a transformation of crystals from a monoclinic form to an orthorhombic form, while transition II is a transition from an orthorhombic phase to a cubic phase. The transition II form is shown in Fig. 7(2): a smooth change of the curve (a prephase state (4)) is observed from 326 K. The temperature of the beginning of the prephase state depends on the sensitivity of the method. Thus, with an increased calorimeter sensitivity, the prephase state is noticeable already from 327 K. The transition I form (monoclinic phase $\rightarrow$ orthorhombic phase) depends on the method of sample preparation. In pressed samples transition I is a narrow single peak; if the crystals are placed in a cuvette loose without being pressed, there is an undulation of transitions I as is shown on a thermogram in Fig. 8(1). So each crystal is characterized by its own T_{kI} value; an interval of ΔT, at which all the crystals pass to the orthorhombic phase, is $\sim 10°$; (i.e., the energy difference between the crystals is of the order of 10^{-4} eV (19.1 cal/mol). The conditions of sample preparation (pressed or loose) do not exert any influence on transition II. The most precise T_{kII} temperature found at a minimal heating rate is 340 K. The influence of cooling temperature T^* on the phase composition of the DMPD crystals was found calorimetrically (Fig. 8). On cooling crystals **1** from $T > T_{\mathrm{kII}}$ and on repeated heating, both phase transitions I and II are observed; i.e., phase I is retained (Fig. 8, compare curve 1 with curve 4 for several samples). If the same sample is cooled from $T_{\mathrm{kI}} < T \ll T_{\mathrm{kII}}$ (curve 2, Fig. 8), then, during repeated heating, transition I disappears (curve 3); i.e., the DNPD crystals correspond to phase **2**. Hence, the orthorhombic phase crystals retain their symmetry down to room temperature (and lower) under the condition that the samples are cooled from $T_{\mathrm{kI}} < T^* < T_{\mathrm{kII}}$. As the cooling rate from $T^* > T_{\mathrm{kI}}$ was ~ 0.2 deg/min, it is quite evident that the orthorhombic phase is preserved not because of its quenching in the low-temperature region, but because this state is kinetically stable. As the calorimetric studies show, at room (and lower) temperatures, the orthorhombic phase crystals are preserved for an infinitely long time. The monoclinic phase in the crystals appears only on cooling of the cubic phase samples. The stability of the orthorhombic phase crystals at room temperatures is confirmed by the calorimetric studies of samples **2** of this substance. Their heating thermogram from 303 to 373 K shown in Fig. 9 from $Q_{\mathrm{II}} = -5.970$ kcal/mol and corresponds with the phase conversion of an initial orthorhombic form into a cubic form (transition I is absent, transition II is observed). Unfortunately, the study of samples **2** was not brought to completion. We did not perform repeated heating of these samples after they were cooled to room temperature from $T^* > T_{\mathrm{kII}}$. However, it is quite probable that on repeated heating we would have seen both transitions, as on cooling the cubic phase crystals the crystals, symmetry

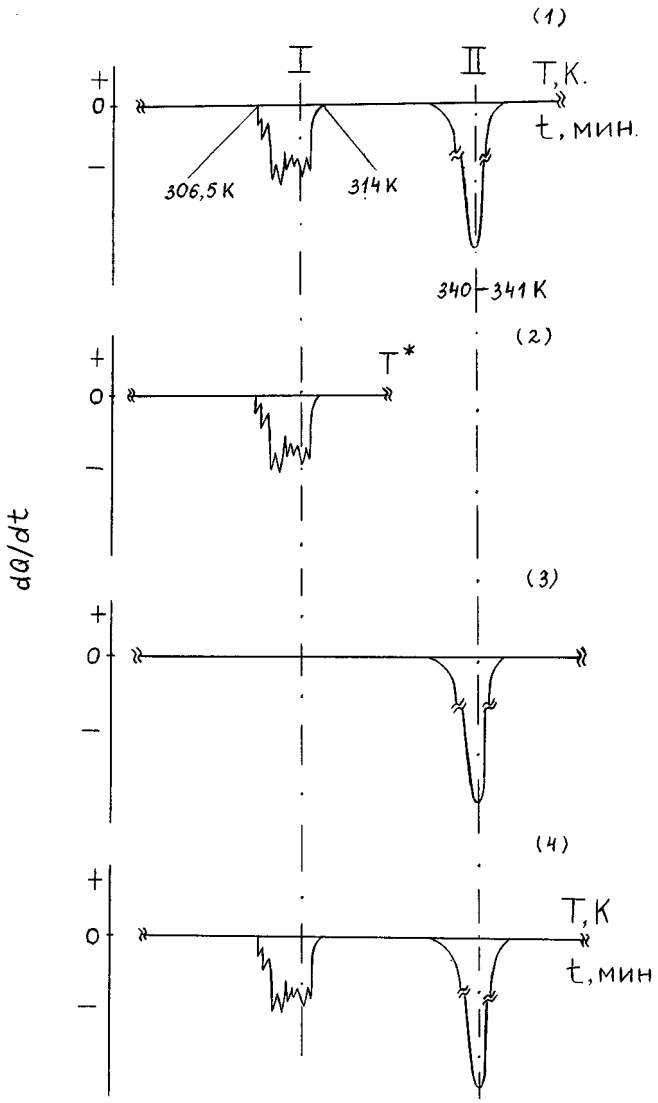

FIG. 8. Thermograms of heating of crystals **1** placed loose in a calorimetric cell: (1) first heating to 373 K, (2) second heating to $T_{kI} < T^* <$ temperature of the transition II beginning, (3) third heating to $T^* \approx 373$ K, and (4) fourth heating to $T \approx 373$ K.

at room temperatures should correspond with the monoclinic phase.

5. *IR Spectra*

IR spectra of 2,2-dinitropropane-1,3-diol in the temperature range 293–370 K were recorded on a Specord 75 IR spectrophotometer in the range 400–4000 cm^{-1} at a spectral slip of no more than 3 cm^{-1} for the range 400–2000 cm^{-1} and 10 cm^{-1} for the range 2000–3700 cm^{-1}. Samples for IR spectroscopy were prepared by crushing the DNPD crystals in a mortar and subsequently pressing them in a mixture with KBr powder. The stability of the initial

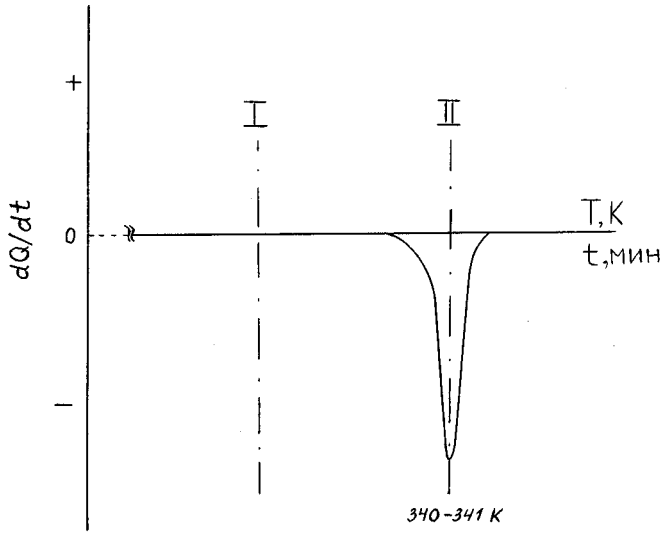

FIG. 9. Thermogram of the heating of crystals **2**. Transition I is absent; for transition II, $Q = -6$ kcal/mol $\pm$ 5%.

phase of DNPD during crushing was checked by preliminary powder diffractogram control. The IR spectra of DNPD allowed us to study the temperature behavior of absorption bands of the symmetric $\nu_S(NO_2)$ stretching vibrations of the nitro group and the O–H group stretching vibrations that account for stable hydrogen bonds. With a temperature rise, both bands undergo significant changes that will be considered separately for each band.

$\nu_S(NO_2)$ Behavior. As expected, two bands are observed in the region of symmetrical stretching vibrations due to the nitro group $\nu_S(NO_2)$ in the IR spectrum of crystals **1** at room temperature. The maxima of the $\nu_S(NO_2)$ absorption are found at 1331 and 1357 cm^{-1}. Judging from the structure of molecule **1** it may be concluded that the low-frequency band is due to the N(2)O(3)O(4) nitro group and the high-frequency one to the N(1)O(1)O(2) nitro group; i.e., the conformational structure of the molecule accounts for both the donation of electron density from the bonding orbitals to the C–O bonds and the population of the N(2)O(3)O(4) nitro group antibonding orbital, which should result in weakening of the N–O bonds. In the N(1)O(1)O(2) nitro group, only the donation of electron density from the bonding orbital to the neighbor nitro group is possible; hence, the maximum absorption of this group lays in the higher-frequency region. With a temperature increase, the band intensity lowers, and the bands become broader, which is followed by transfer of the intensity to a low-frequency band so that at 336.6 K in the spectrum there is a broad band with an absorption maximum at 1336 cm^{-1} and a shoulder at 1350 cm^{-1} (Fig. 10). It is of interest that, beginning from 313.8 K (i.e., after the first phase transition) up to the temperature of the second

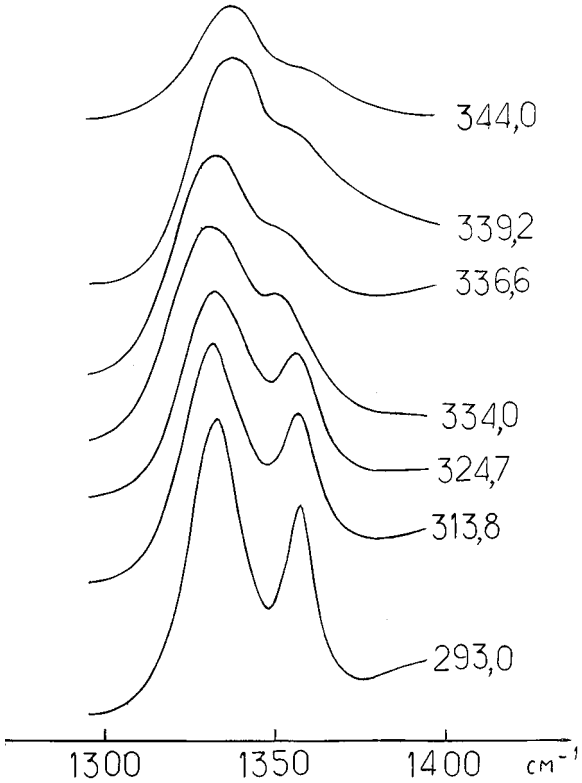

FIG. 10. Temperature dependence of the DNPD IR spectrum in the region of symmetric stretching vibrations of the nitro groups.

phase transition, both bands shift to the low-frequency region; after the second phase transition at 339.2 K, the position of the maximum returns to the same point. Beginning from 313.8 K, the DNPD molecule conformation corresponds to phase II, and further temperature increases should lead to decreasing the intermolecular attractive interactions stabilizing the molecule conformation, and further to a transition of the molecule to a new state leading to increased steric strain in the dinitromethyl fragment. It is probable that a difference in the N–O bond lengths of the nitro groups revealing itself after the first phase transition may account for the shifting of the band maximum in this temperature region. The temperature dependence of the low-frequency band breadth in the range 300–330 K is satisfactorily described by the following expression ($6 \simeq 8$): $\Delta\nu(T) = \Delta\nu_1 + \Delta\nu_2(T)$, where $\Delta\nu_1 = 5.1\ \mathrm{cm}^{-1}$; $\Delta\nu_2(T) = \Delta\nu_2^0\ \mathrm{e}^{-E/RT}$; $E = 3.81$ kcal/mol; $\lg[\Delta\nu_2(\mathrm{c}^{-1})] = 14.25$.

At about 333 K, there is a jumpwise increase in $\Delta\nu$ (Fig. 11), which can be associated with the second phase transition. Most likely, a narrow band at 1357 cm^{-1} adjustable with respect to the N(1)O(1)O(2) nitro group characterizes a less labile nitro group, while a broad band at 1331 cm^{-1} relates to the more labile N(2)O(3)O(4) nitro group (phase I). With a temperature increase, the portion of the less labile NO_2 groups decreases but their lability grows,

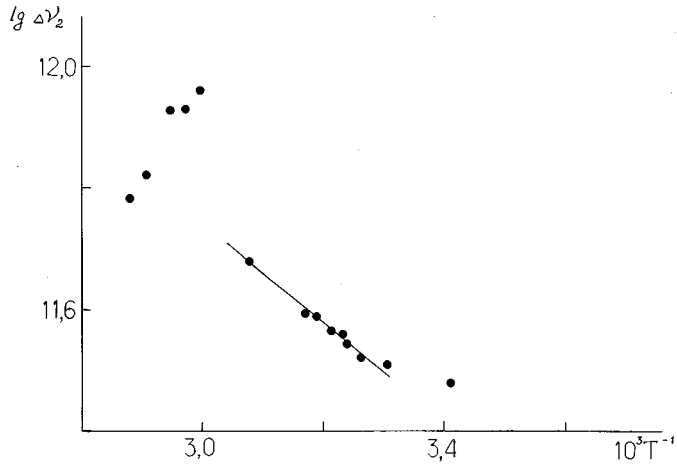

FIG. 11. Temperature dependence of the low-frequency component of the DNPD $\nu_S(NO_2)$ doublet in Arrhenius coordinates.

which is reflected in the broadening of the high-frequency $\nu_S(NO_2)$ component. An anomalously high value of preexponential multiplier $\Delta\nu_2^0 = 10^{-14.25}\,\mathrm{s}^{-1}$ may be related to an increased entropy due to releasing of the rotational movements in the transition state.

Behavior of OH stretching vibrations. In the region of O–H stretching vibrations of the compound **1** IR spectrum at low temperature (293 K) there is a complex band with a maximum at 3298 cm^{-1}. Splitting of the contour of this band into individual Foygt components (Fig. 12) leads to three bands, two of which (at 3354 and

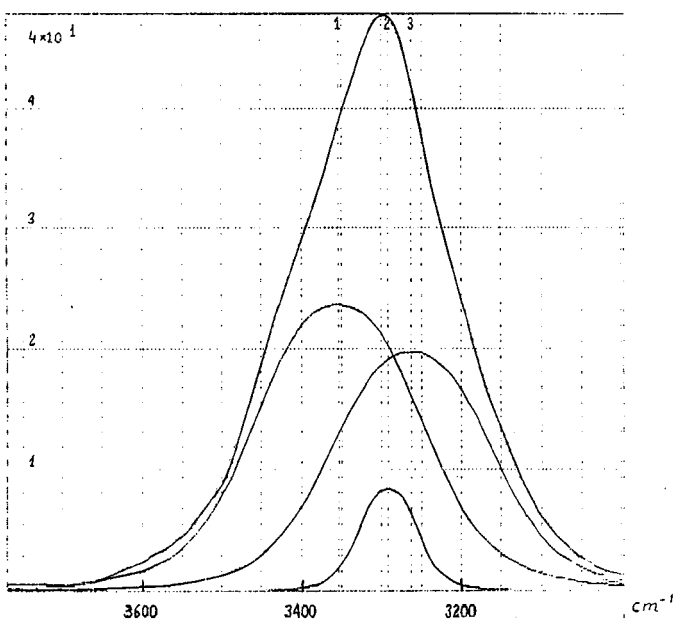

FIG. 12. Structure of the DNPD ν(OH) band at 289 K.

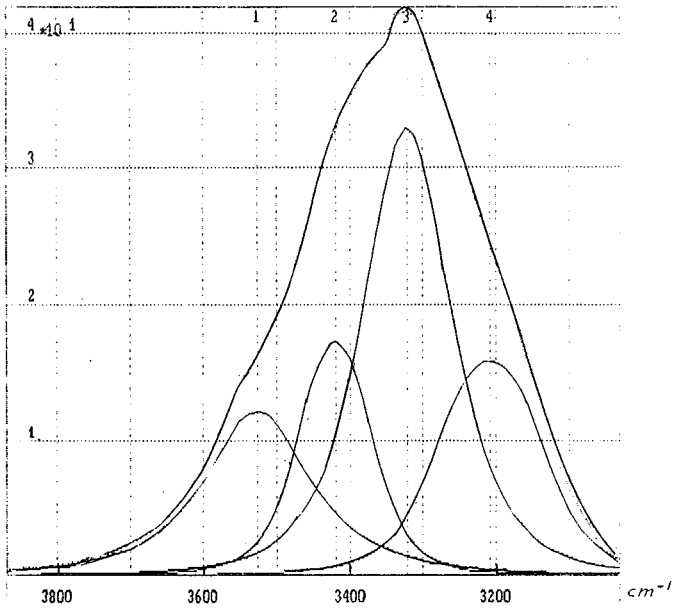

FIG. 13. Structure of the DNPD ν(OH) band at 326 K.

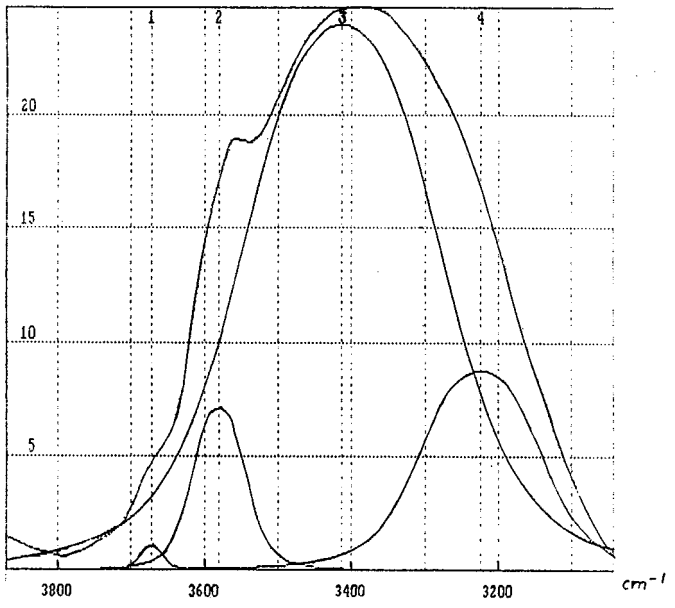

FIG. 14. Structure of the DNPD ν(OH) band at 340 K.

3263 cm^{-1}) have close integral intensities and belong to the stable hydrogen bonds observed in structure **1**. The nature of the third (weak and narrow) band at 3292 cm^{-1} is unclear; it may likely be a composite or resonance band. All three components have a Gaussian form. As the temperature increases, there is a gradual change in the contour shape in the region of 3000–3300 cm^{-1}, and at 326 K (after the first transition) the bands due to hydrogen bonds observed in the IR spectrum at 293 K are absent. The complete contour is a superposition of four new Foygt components whose forms cannot be described by the Gaussian function (Fig. 13). The considerable contribution of a Lorentz component in this case suggests a significant contribution of the dynamic factors in the broadening of the O–H stretching vibrations bands. In the vicinity of 335 K (second phase transition), a jumpwise change in the IR spectrum in the region of the O–H stretching vibrations is observed. A new contour is described by four purely Gaussian components, one of which (at 3672 cm^{-1}) corresponds with the practically free OH groups, while the other three correspond with hydrogen bonds of different stability (Fig. 14). It should be noted that, with a temperature rise from 289 to 344 K, the mean energy of hydrogen bonds in the structure falls continuously, which is reflected in the shift of the spectral envelope centre to the region of high frequencies.

6. *Temperature NMR Investigations of the DNPD Crystals in the Solid Phase*

The NMR pulse method in the solid phase can give useful information on the mobility of structural elements when studying the structural and dynamic changes in the DNPD crystals. As judged from the character of the relaxational decay of the proton signals (FID) and its temperature dependence, the mobility of the proton-containing fragments in the DNPD molecules was determined. The NMR investigations were conducted on a pulse (PU 2303) spectrometer with a frequency of 60 MHz in the temperature range 293–378 K with an interval of 5°. The temperature accuracy was $\pm 1^0$. Depending on the temperature interval and their own characteristics the decay curves could be divided into three groups. The first group—293–323 K (Fig. 15)—is characterized by the absence of the temperature effect on the decay; the second group—323–343 K (Fig. 16)—demonstrates a complicated character of the decay, in which approximately three separate components are observed; and

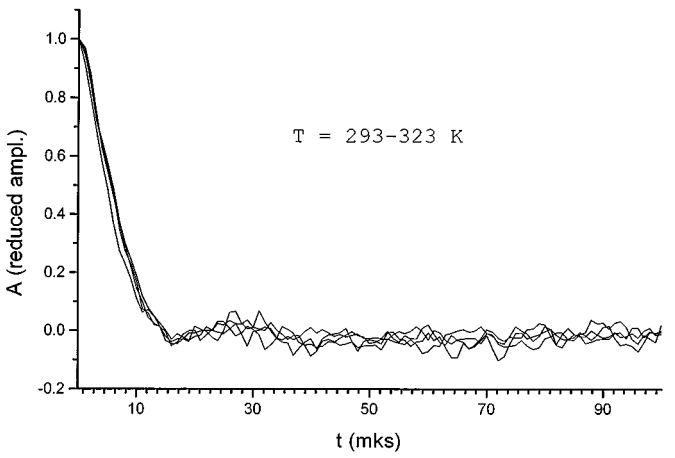

FIG. 15. Curves of the protons' signal decay in crystals **1** (293–323 K, the first group of curves).

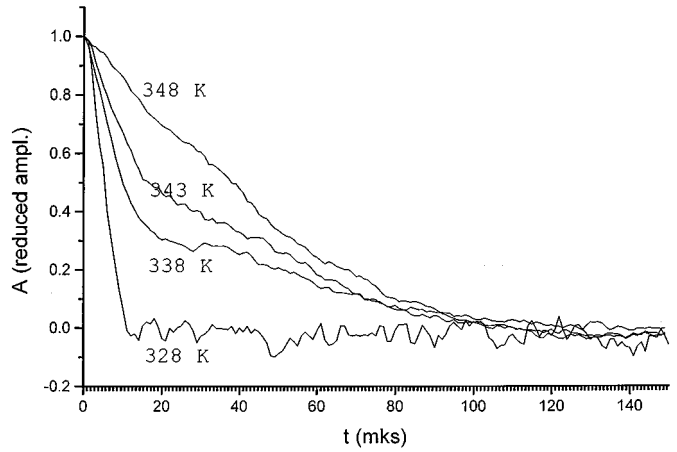

FIG. 16. Curves of the protons' signal decay (FID) in crystals **1** (323–343 K, the second group of curves).

in the third group—342–378 K (Fig. 17)—the decay curves have a monotonic exponential appearance typical of a uniform noncomplicated movement. The temperature regions in the vicinity of the two phase transitions are not considered because of the uncertainty of the beginning of the transitions in these regions. As is known, the pulse NMR method in the solid phase records movements with frequencies that are several orders of magnitude slower than, e.g., the frequencies of infrared vibrations. In the DNPD crystals the observed decay is determined by the mobility of protons in the $(CH_2OH)_2$ groups, which is connected with the mobility of the groups themselves. In them, the $-CH_2$ lability depends on the movements of the $-CH_2OH$ groups about the C–C bond. This movement may overlap with the process of cleavage and restoration of two different systems of hydrogen bonds, one of them oriented along the *c* axis and the second linking chains in pairs. The variation of the proton mobility with a temperature rise can be represented,

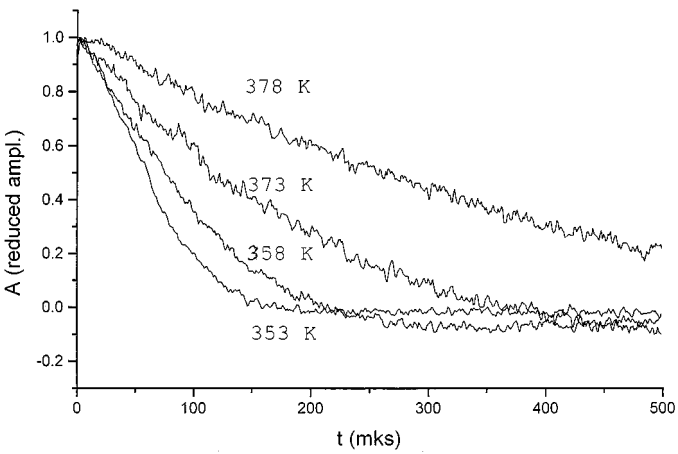

FIG. 17. Curves of the protons' signal decay (FID) in crystals of **1** (343–378 K, the third group of curves).

using the NMR data, as follows. From room temperature to $\sim$323 K, the low-frequency movements of the CH_2OH groups are practically absent, which is confirmed by the temperature independence of the decay curves of the proton signals (the first group of decay curves, Fig. 15). The second group of decay curves (325–343 K) is indicated by the beginning of cleavages and restorations of the hydrogen bonds (probably, through proton exchanges) in two systems, which is confirmed by the components of the decay curves and the beginning of the CH_2OH turning about the C–C bond. These processes at the beginning of the fragments' movement are characteristic of an appearance of a prephase state of transition I. The decay rate constant found at the initial section of this temperature region (Fig. 16) is $K(2)_{\mathrm{BEG}} = 5.5\,\mathrm{e}^{-4}\ \exp(12265/RT)\,\mathrm{s}^{-1}$. When the temperature approaches the point of phase transition II from an orthorhombic phase into a cubic phase, rotating molecules may appear if their hydrogen bond systems are destroyed, hence the change in the form of the decay curve and its resemblance to an exponential form. After phase transition II is over, all the molecules pass to a rotating state. In this case, the short-lived hydrogen bonds are retained and their arrangement in the crystal lattice becomes disordered. Such a disordered rotation of molecules with periodic "hooking" is evidently characteristic of the plastic crystal state. The proton signal decay curve (Fig. 17) becomes uniform, i.e., describes the movements of only one type; it acquires a more exponential appearance and the decay rate constant reaches the following value:

$$K(3) = 3.86 \times 10^{-6}\ \exp(15550/RT)\,\mathrm{s}^{-1}.$$

This value may be effective and may exceed the lattice energy value due to successive overcoming of the "hooking" barriers.

RESULTS AND DISCUSSION

A complex approach has been applied in this work when different methods complementing each other were used to study different aspects of the DNPD structural dynamic properties. The data obtained allow us to describe the general aspects of the structural–dynamic variations both of separate molecules and of the crystal structure as a whole. With a temperature increase, the conformational change in the molecules passes in the direction of the conversions **1** → phase transition I → **2** → phase transition II → **4**, where **1** and **2** are the phases described above, and **4** is the cubic phase formed by chaotically rotating molecules. As is clear from the description of the molecular structure, the temperature changes in the conformation begin from rotations of the CH_2OH groups about the C–C bonds, and then a significant rearrangement takes place in the more energy-consuming fragments of the NO_2 groups, which is repre-

sented by the changes in the interaction between them and with the C–O bonds, all this leading to transition I. The value of the conformational conversions barrier in molecule **1** is comparable with the energy of the hydrogen bonds in the crystal structure, while the energy advantage of structure **1**, as compared to structure **3**, is comparable with the thermal effect of phase transition I. It should be noted here that in different crystals of phase **1**, because of differences in their defectiveness, the concentration of the DNPD molecules with changed conformation is probably different; this may result in some interval ΔT_{kI} of temperatures T_k mentioned above. The phase transition **1** → **2** begins on defective spots of the crystals, probably because of increased concentration of nonequilibrium defects of the dislocation type and a stimulating effect of mechanical stresses. A prolonged front of propagating conversion observed by us in a hot stage under an optical microscope may be explained by the arising of new phase nuclei in the volume of the initial phase, their fast growth, and their subsequent coalescence. In this case, the role of the mechanical stresses arising due to difference of the phase volumes may be significant. In the new structure **2**, the character of nonbonded interactions in the molecule is different: the interaction between the nitro groups is weakened and the interaction of each of them with separate C–O bonds is enhanced. The observed overcooling of the orthorhombic phase with a temperature decrease may take place because the formation of an orthorhombic phase on heating leads to the formation of a nondefective crystal (phase transition **1** → **2** may be accompanied by annihilation of nonequilibrium defects), while, with a temperature decrease to T_{kI} and lower, a considerably larger energy expenditure is required to form nuclei of a new phase than it is required in a defective crystal. As phase transition I turns **1** into **2**, it may be assumed that growing the DNPD crystals from a solution in DCE at a temperature close to T_{kI}, but lower than this, leads to phase transition I under "milder" conditions leading to formation of phase **3** with a structure almost identical to that of phase **2**. This fact makes us believe that the DNPD molecules' conformation depends on the temperature in the solution as well, which was confirmed by growing a layer of plastic crystal under a microscope at ~ 328 K (lower than T_{kII}); in this case the material had a cubic symmetry as it was not optically active under a polarized light and passed to an optically active form after it was cooled to room temperature. These observations show that the conformation of the DNPD molecules in the DCE solution is dependent on temperature and should evidently correspond to conformations **1**, **2** and **3**. This question, however, needs further investigation.

In the solid phase, the DNPD crystals experience phase transition II leading to cubic phase **4** formed by rotating molecules. In their rotation, the molecules form short-lived hydrogen bonds with each other. The body-centered cubic lattice of the DNPD crystals is arranged so that a short contact between the rotating spheres takes place along the body cube diagonal. This is probably the direction in which the bridges of the hydrogen bonds arising for a short time lie. Thus, the crystal lattice of the DNPD crystals has systems of stable hydrogen bonds in structures **1**, **2**, and **3** and unstable bonds in structure **4**. The differences in phases **2** and **3**, as mentioned above, are inconsiderable. However, structure **3** clearly demonstrate a difference in the N–O bonds lengths, 1.21(1) and 1.24(1) Å, in each nitro group which confirms their nonequivalence.

The volume of the DNPD molecule, $V_M^{(X)}$, is different. Thus for **1**, $V_M^{(1)} = 162.46$ Å, after phase transition I in orthorhombic phase **2**, $V_M^{(2)} = 166.97$ Å^3; in structure **3**, $V_M^{(3)} = 166.82$ Å^3 (the packing coefficient is 1). So with temperature increasing, the volume also increases and the lattice becomes more "loose." After phase transition II in the body-centered cubic lattice, the rotating molecule size (the "body of rotation" volume) is $V_M^{(4)} = 333$ Å^2. During rotation, the atomic coordinates are not recorded and, on the basis of the IR spectra data, it may be assumed that the NO_2 groups' configuration is determined only by the intermolecular interactions, while the OH groups find themselves mostly in a "free" state forming hydrogen bonds with the chaotically rotating neighbors. The specific feature of the plastic crystal in a cubic phase is that it is formed by the rotating molecules has low X-ray density (large phase volume) and has no nonequilibrium defects of the dislocation type. The phase transition to a cubic phase is prepared in the orthorhombic volume first separately and, then, arranged in the coherent scattering regions rotating molecules, resulting in the formation of a loose plastic structure of a cubic crystal. The reverse transition is connected with the overcooling and subsequent catastrophic rearrangement of the lattice structure, which is accompanied (because of a sharp change in the phase volume) by the arising of defective, mechanically stressed areas in the crystal. Such conditions favor the formation of the most stable phase—monoclinic, omitting a not very stable orthorhombic one. The investigations performed have shown that both the conformation of separate molecules and the crystal structure as a whole undergo significant changes with changing temperature with both the DNPD and other molecular crystals (1, 2), which must be taken into consideration when examining the questions of their reactivity, in particular, thermostability and thermodecomposition. In this case, the process will be determined by the specific features of the structure of the molecular crystal and will demand a special study in each separate case.

ACKNOWLEDGMENT

This work was supported by the Russian Foundation for Basic Research (Grant 00-03-32885).

REFERENCES

1. N. I. Golovina, A. N. Titkov, A. V. Raevskii, and L. O. Atovmayn, *J. Solid State Chem.* **113,** 229–238 (1994).
2. N. I. Golovina, A. V. Raevskii, B. S. Fedorov, I. G. Gusakovskaya, R. F. Trofimova, and L. O. Atovmyan, *J. Solid State Chem.* **137,** 231–241 (1998).
3. N. I. Golovina, L. N. Leksina, R. F. Trofimova, and L. O. Atovmyan, *Zh. Strukt. Khim. AN SSSR.* **2,** 172–174 (1988).
4. H. Feuer, J. Bachman, and I. Kisperski, *J. Am. Chem. Soc.* **73,** 1360 (1951).
5. J. Koo and N. L. Allinger, *J. Am. Chem. Soc.* **99,** 975–979 (1977).
6. A. I. Rakov, *Opt. Spektrosk.* **7,** 202 (1959).
7. V. I. Vettegren, I. V. Dreval, V. E. Korsukov, and I. I. Novak, *Vysokomol. Soedin. Ser. B* **12,** 680 (1970).
8. B. Coen and S. Weiss, *J. Phys. Chem.* **88**(14), 1359–3162 (1984).